



FULL PAPER

A novel five-step synthetic route to 1,3,4-oxadiazole derivatives with potent α -glucosidase inhibitory potential and their in silico studies

Muhammad Iftikhar¹ | Shahnawaz¹ | Muhammad Saleem¹ | Naheed Riaz¹ | Aziz-ur-Rehman² | Ishtiaq Ahmed³ | Jameel Rahman¹ | Muhammad Ashraf¹ | Muhammad S. Sharif¹ | Shafi U. Khan⁴ | Thet T. Htar⁴

¹Department of Chemistry, Baghdad-ul-Jadeed Campus, The Islamia University of Bahawalpur, Bahawalpur, Pakistan

²Department of Chemistry, Government College University Lahore, Lahore, Pakistan

³Institute for Biological Interfaces (IBG-1), Karlsruhe Institute of Technology (KIT), Karlsruhe, Germany

⁴School of Pharmacy, Monash University Malaysia, Subang Jaya, Malaysia

Correspondence

Naheed Riaz, Department of Chemistry, Baghdad-ul-Jadeed Campus, The Islamia University of Bahawalpur, Bahawalpur 63100, Pakistan.

Email: nrch322@yahoo.com; nrch322@iub.edu.pk

Abstract

A series of new *N*-aryl/aralkyl derivatives of 2-methyl-2-[5-(4-chlorophenyl)-1,3,4-oxadiazole-2ylthiol]acetamide were synthesized by successive conversions of 4-chlorobenzoic acid (**a**) into ethyl 4-chlorobenzoate (**1**), 4-chlorobenzoylhydrazide (**2**) and 5-(4-chlorophenyl)-1,3,4-oxadiazole-2-thiol (**3**), respectively. The required array of compounds (**6a–n**) was obtained by the reaction of 1,3,4-oxadiazole (**3**) with various electrophiles (**5a–n**) in the presence of DMF (*N,N*-dimethylformamide) and sodium hydroxide at room temperature. The structural determination of these compounds was done by infrared, ¹H-NMR (nuclear magnetic resonance), ¹³C-NMR, electron ionization mass spectrometry, and high-resolution electron ionization mass spectrometry analyses. All compounds were evaluated for their α -glucosidase inhibitory potential. Compounds **6a**, **6c–e**, **6g**, and **6i** were found to be promising inhibitors of α -glucosidase with IC₅₀ values of 81.72 ± 1.18, 52.73 ± 1.16, 62.62 ± 1.15, 56.34 ± 1.17, 86.35 ± 1.17, 52.63 ± 1.16 μ M, respectively. Molecular modeling and ADME (absorption, distribution, metabolism, excretion) predictions supported the findings. The current synthesized library of compounds was achieved by utilizing very common raw materials in such a way that the synthesized compounds may prove to be promising drug leads.

KEYWORDS

4-chlorobenzoic acid, mercapto-*N*-aryl/aralkyl propionamide oxadiazoles, *N*-substituted-2-bromopropionamide, α -glucosidase inhibition

1 | INTRODUCTION

Oxadiazoles are classified as five-membered heterocyclic ring systems containing one oxygen and two nitrogen atoms in the ring system. Amongst the four possible isomers of oxadiazoles, the isomer 1,3,4-oxadiazole is the most widely studied.^[1,2] The capability of the 1,3,4-oxadiazole nucleus to undergo a variety of chemical reactions has made it a medicinal backbone, and thus it has drawn attention for consideration in a wide range of applications. 1,3,4-Oxadiazole

nucleus is present in several drug molecules. For example, furamizole is an antibiotic,^[3] nesapidil is a calcium channel blocker and a vasodilating agent,^[4] raltegravir is anti-HIV and inhibits HIV integrase enzyme,^[5] and tiadazosin is an antihypertensive drug (Figure 1).^[6] Several other derivatives of oxadiazoles have shown biological activities, which include antimicrobial,^[7–9] anti-inflammatory,^[10] antitubercular,^[1,11] antioxidant,^[12,13] anticancer,^[14–17] anti-proliferative,^[18] antiviral,^[19,20] anticonvulsant,^[21,22] antiacetylcholinesterase,^[23] antihistone deacetylase,^[24] antixanthine oxidase,^[25]

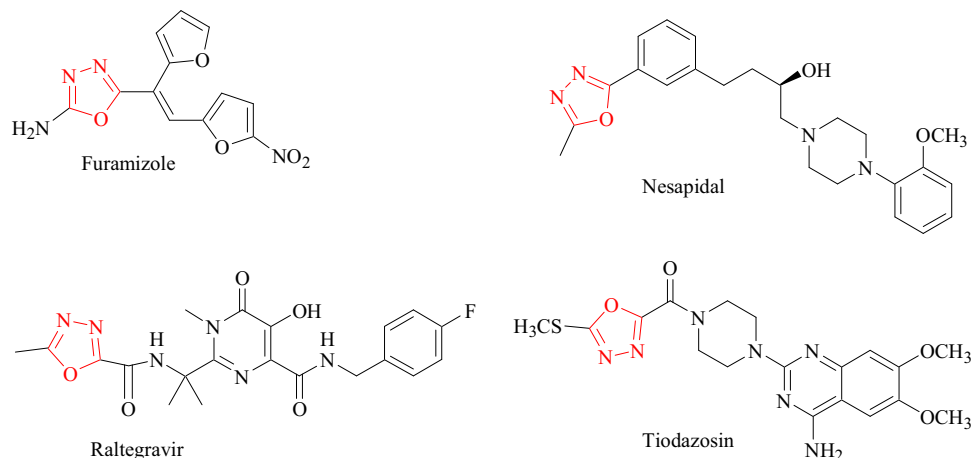


FIGURE 1 Available drugs containing oxadiazole moiety in their structures

potent inhibition of Dengue and West Nile virus NS2B/NS3 proteases,^[26] antidiabetic,^[27,28] 5-HT₄ receptor partial agonistic,^[29] benzodiazepine receptor agonistic,^[30] and analgesic.^[31,32] It has been observed that alkyl or aryl halide derivatives of oxadiazoles have better biological activities than the unsubstituted 1,3,4-oxadiazole.^[33] Besides, it is reported that compounds bearing 1,3,4-oxadiazole core are good inhibitors of the enzyme α -glucosidase.^[34]

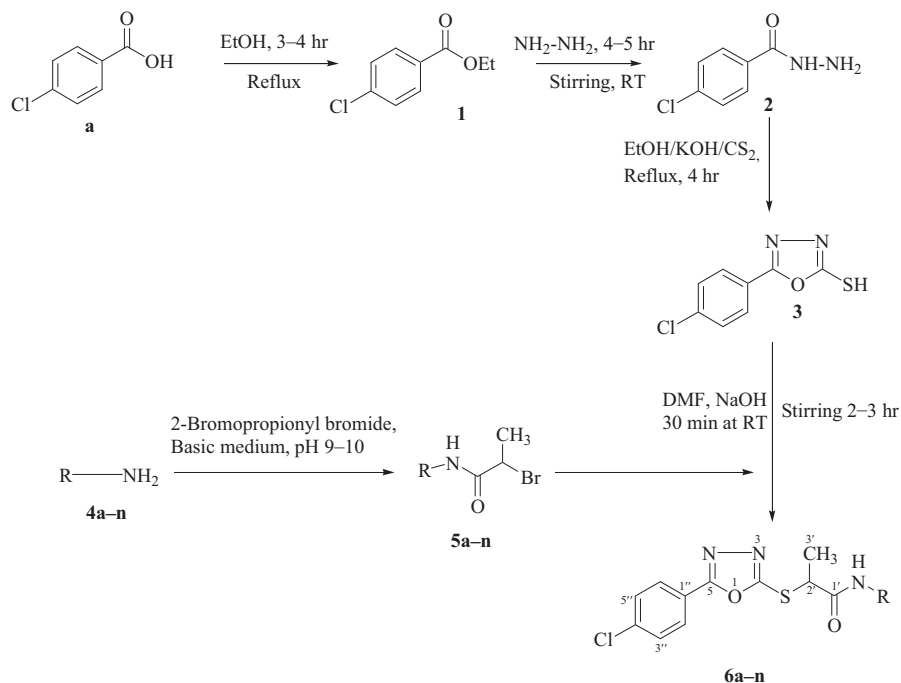
The enzyme α -glucosidase (EC.3.2.1.20) is produced by the brush border of small intestine. It catalyzes hydrolysis of α -1 \rightarrow 4-glycoside bond in oligosaccharides to produce glucose. The absorption of

glucose causes postprandial hyperglycemia in diabetes mellitus type 2 patients.^[35] Acarbose, voglibose, and miglitol are known antidiabetic drugs, which inhibit α -glucosidase activity. However, these drugs have several side-effects including diarrhea, abdominal discomfort, and so on. Thus, there is a significant need to keep searching for new antidiabetic drugs with minimum side-effects.^[35] The present study focuses on the synthesis, characterization, and in vitro enzyme inhibition along with docking studies and the absorption, distribution, metabolism, and excretion (ADME) properties of compounds in search for potent antidiabetic lead molecules.

TABLE 1 R-groups in aryl/alkyl substituted amines

Compound	-R	Compound	-R	Compound	-R
a		f		k	
b		g		l	
c		h		m	
d		i		n	
e		j		-	-

SCHEME 1 Synthesis of *N*-substituted 5-(4-chlorophenyl)-1,3,4-oxadiazole-2-yl-sulphonyl-2"-methylacetamides (**6a-n**)



2 | RESULTS AND DISCUSSION

2.1 | Chemistry

N-(Aryl/aralkyl)-2-methyl-(2-[5-(4-chlorophenyl)-1,3,4-oxadiazole-2-yl-thiol]acetamides (**6a-n**) with their substituted aryl/aralkyl groups (Table 1) were synthesized as shown in Scheme 1. The synthesized compounds were screened against yeast α -glucosidase and were found to be good inhibitors of the enzyme (Table 2).

The target compounds **6a-n** were synthesized in a number of steps. First, the two main precursors 5-(4-chlorophenyl)-1,3,4-oxadiazol-2-thiol (**3**) and 2-bromo-*N*-[aryl/aralkyl]propionamide (**5a-n**) were prepared

separately. Compound **3** was prepared starting with reflux of 4-chlorobenzoic acid (**a**) in ethanol catalyzed by concentrated H_2SO_4 to get the corresponding ethyl ester (**1**), which upon reaction with hydrated hydrazine in methanol produces carbonyl dihydrazide (**2**), which in turn was refluxed with carbon disulfide in the presence of ethanolic potassium hydroxide to get the cyclized product 5-(4-chlorophenyl)-1,3,4-oxadiazol-2-thiol (**3**). The other precursors (**5a-n**) of the target compounds were prepared through coupling of aryl/aralkyl amines (**4a-n**) with 2-bromopropionyl bromide in basic media (pH 9–10). The target compounds (**6a-n**) were finally produced in a good yield by reacting precursor **3** with electrophiles 2-bromo-*N*-[aryl/aralkyl]propionamide (**5a-n**; Scheme 1). Structures of compounds **6a-n** were established through IR, 1H -NMR (nuclear magnetic resonance) and ^{13}C -NMR spectroscopy, electron ionization mass spectrometry (EI-MS), and high-resolution electron ionization mass spectrometry (HR-EI-MS).

TABLE 2 α -Glucosidase inhibition potential of compounds **6a-n**

Compound	Inhibition (%) at 0.5 mM	IC ₅₀ (μ M)
6a	97.57 \pm 1.24	81.72 \pm 1.18
6b	75.35 \pm 1.26	275.45 \pm 1.21
6c	96.72 \pm 1.24	52.73 \pm 1.16
6d	94.64 \pm 1.26	62.62 \pm 1.15
6e	95.32 \pm 1.25	56.34 \pm 1.17
6f	74.84 \pm 1.29	275.72 \pm 1.25
6g	91.52 \pm 1.23	86.35 \pm 1.17
6h	86.42 \pm 1.28	124.52 \pm 1.24
6i	96.36 \pm 1.25	52.63 \pm 1.16
6j	85.38 \pm 1.23	124.32 \pm 1.19
6k	68.45 \pm 1.21	–
6l	38.45 \pm 1.19	–
6m	17.45 \pm 1.13	–
6n	24.45 \pm 1.16	–
Acarbose	65.73 \pm 1.93	375.82 \pm 1.76

2.1.1 | Spectral characterization of compound **6a**

The IR spectrum of compound **6a** showed absorption bands for several functions as 3,020 (Ar-H), 2,920 (C-H), 1,696 (C=O), 1,597–1,535 (C=C, C=N), 1,237 (C-O), 1,063 (C-N) cm^{-1} . Resonances of a doublet methyl at δ 1.73 ($J = 6.7$ Hz) and a methine quartet at δ 4.52 ($J = 6.7$ Hz) in 1H -NMR spectrum were attested for *S*-substituted propamide function in **6a**. The 1H signals for *p*-chlorophenyl attached to 1,3,4-oxadiazole moiety appeared as two doublets at δ 7.48 (2H, $J = 8.5$ Hz), 7.91 (2H, $J = 8.5$ Hz), whereas the signals for the *N*-phenyl group displayed their position at δ 7.07–7.15 (5H, m). Quaternary carbons of the oxadiazole ring resonated at δ 165.1 (C-5) and 165.3 (C-2) in the ^{13}C -NMR spectrum, whereas carbonyl carbon of amide function displayed its position at δ 168.1 (C-1). The signals due to carbons of 4-chlorophenyl moiety were observed at δ 141.1 (C-4'), 138.4 (C-1'), 129.0 (C-2',6'), and

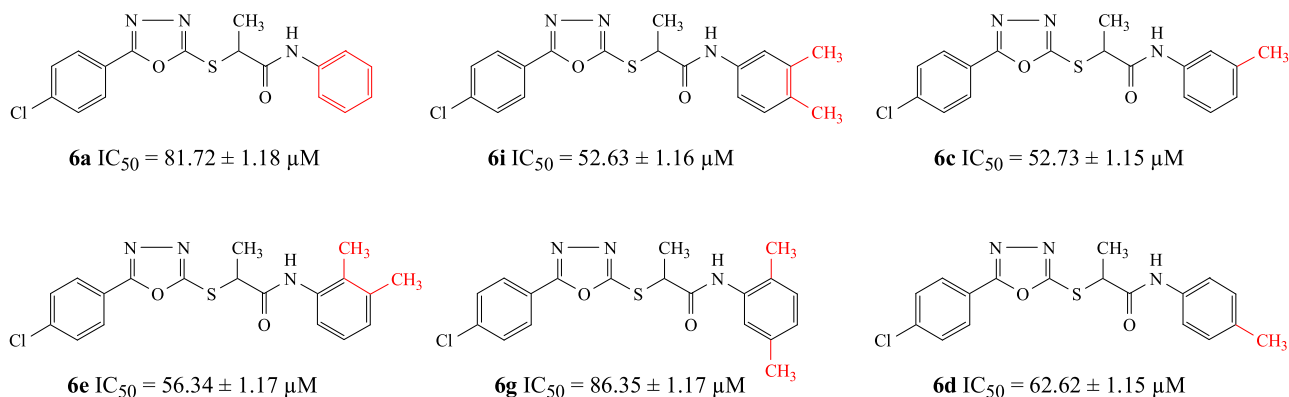


FIGURE 2 Comparison of SAR (structure–activity relationship) of the most active compounds

124.0 (C-3",5"). The *N*-phenyl group appeared at δ 138.4 (C-1"), 119.8 (C-2"), 136.2 (C-3"), 137.7 (C-4"), 129.6 (C-5"), 129.0 (C-6"). The EI-MS spectrum of **6a** afforded the molecular ion peak [M]⁺ at *m/z* 359.3 with some characteristic fragments at *m/z* 268.0 and 111.0 due to *p*-aminophenylloxadiazole and chlorophenylloxadiazole moieties, respectively. This spectral analysis led to the structure of **6a**; along with this compound, the data of other analogues **6b–n** have been provided in the experimental part.

2.2 | α -Glucosidase inhibitory activity

As yeast α -glucosidase shows structural and functional resemblance with the human α -glucosidase, it was used for routine screening of molecules possessing antidiabetic potential. All the synthesized oxadiazole amides (**6a–n**) showed promising inhibitory potential against α -glucosidase with IC₅₀ values between 52.63 ± 1.16 and 275.72 ± 1.25 μM, which are all comparable with the inhibitory potential (IC₅₀ 375.82 ± 1.76 μM) of standard acarbose (Table 2). The products derived from phenylamine showed significant activity, **6a** with IC₅₀ = 81.72 ± 1.18 μM. The analysis of the structural features and activity potentials reveals that the presence of phenyl or mono- or dimethylated phenyl amines has a strong pharmacophoric effect in enhanced antiglycosidase activity. Among the substituted phenyl amines, the target compounds derived from mono- or di-substitution at *meta*-positions showed significant α -glucosidase inhibitory potential, that is, **6i** (IC₅₀ 52.63 ± 1.16 μM), **6c** (IC₅₀ 52.73 ± 1.15 μM), **6e** (IC₅₀ 56.34 ± 1.17 μM), and **6g** (IC₅₀ 86.35 ± 1.17 μM; Figure 2). Besides, *para*-methylated phenylamine-derived compound **6d** also displayed potent inhibitory activity with an IC₅₀ value of 62.62 ± 1.15 μM. However, the compounds derived from mono-substituted ethyl or ethoxy amines (**6k–n**) were found inactive. The decrease in enzyme inhibition potential is observed as **6i** = **6c** > **6e** > **6d** > **6a** > **6g**. Compounds **6h** and **6j** showed good and **6b** and **6f** showed moderate enzyme inhibition profiles.

TABLE 3 Ramachandran plot analysis of *Saccharomyces cerevisiae* α -glucosidase

Favored region	Allowed region	Outlier region
569 (98.1%)	11 (1.9%)	0 (0.0%)

2.3 | Homology model of *Saccharomyces cerevisiae* α -glucosidase

The homology model three-dimensional (3D) structure of the target *S. cerevisiae* α -glucosidase was constructed. The sequence alignments between isomaltase from *S. cerevisiae* (PDB ID: 3A4A) and *S. cerevisiae* α -glucosidase showed that there was a high sequence identity and a sequence similarity of 71.4% and 86.9%, respectively. The crystal structure of isomaltase was selected as a template structure and downloaded from the Protein Database Bank (PDB). Twenty different model structures were built, and on the basis of the DOPE score, the best model was selected. Validation of the model structure was performed via Ramachandran plot and showed that about 98.1% residues

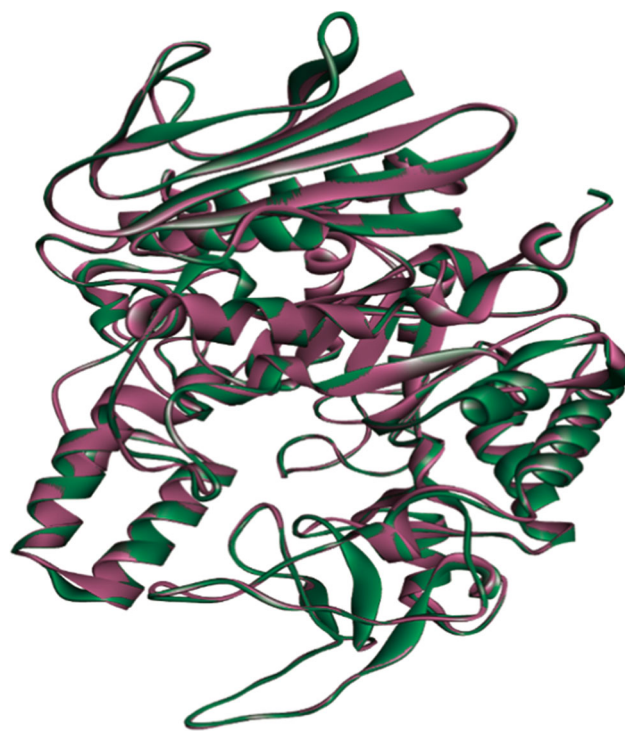


FIGURE 3 Three-dimensional overlapped orientation of template structure (PDB: 3A4A in green color) superimposed on modeled structure of α -glucosidase (pink color)

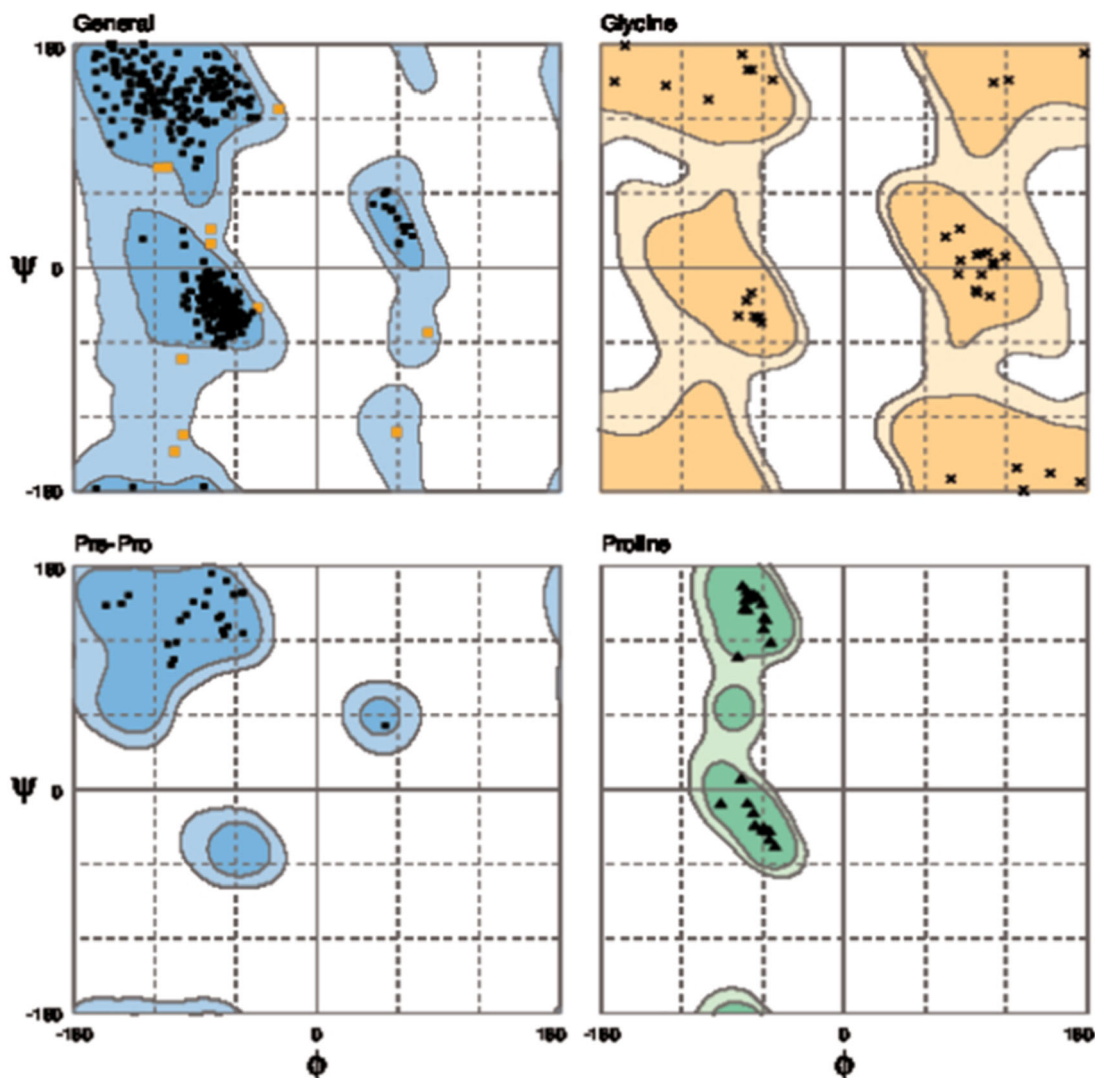


FIGURE 4 Validation of the homology model of α -glucosidase using the RAMPAGE Ramachandran plot

were in the favored region, 1.9% residues in the allowed region, whereas no outlier residue was found in structure a (Table 3) which indicated the good stereochemistry of the model structure and it was found fit for further docking studies. The 3D overlapped structure of the template structure and the modeled structure of α -glucosidase and the Ramachandran plot are shown in Figures 3 and 4.

2.4 | Molecular docking studies

Molecular modeling is widely used to illustrate the potential interaction modes of the active inhibitors binding to the protein target. Molecular docking was performed on the synthesized compounds (6a–n) to identify that plausible binding mode can explain their inhibitory activity. To validate the docking protocol, first-bound cocrystal ligand, α -D-glucose, was docked in the modeled structure, which exhibited a very good root-mean-square deviation of 0.73 (Figure 5), reflecting the crystal and redocked α -D-glucose within active site of target structure. Figure 5 shows



FIGURE 5 Validation of docking protocol, cocrystal bound α -D-glucose (green) and redocked α -D-glucose (cyan) in model structure (RMSD = 0.73)

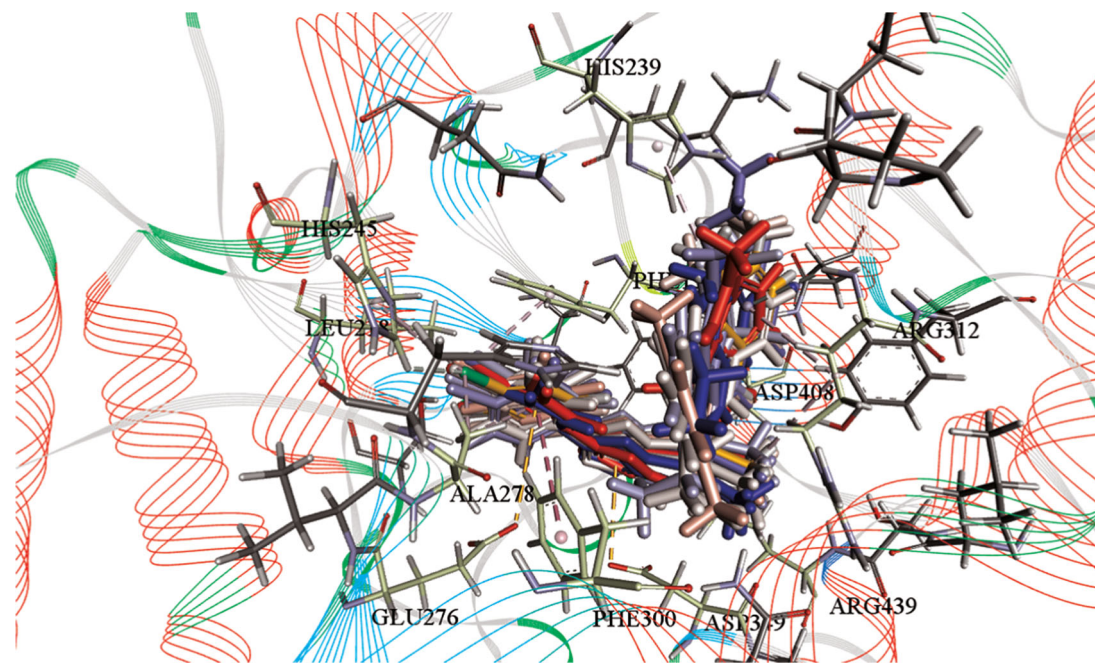


FIGURE 6 Orientation of all docked compounds **6a–n** within the active site of modeled structure of yeast α -glucosidase. Different interacting amino acids within the active site of α -glucosidase are shown in stick form

the overlapped binding orientation of all docked compounds within the active site of modeled structures. The best position was selected based on cluster analysis of docking-binding position having the highest probability with reference to stability of the ligand–substrate complex. Docking showed that all compounds were docked well within the active site of the target enzyme (Figure 6) and the Chemgauss4 score of docked compounds is shown in Table 4. Difference in binding interactions was due to the attached side chain differences in the corresponding compounds. Detailed analysis of binding interaction of potent compounds **6c**

TABLE 4 Chemgauss4 score of compounds **6a–n** against α -glucosidase modeled structures

Sr. No.	Compound	Chemgauss4 score
1	6a	-11.60
2	6b	-10.85
3	6c	-10.42
4	6d	-11.63
5	6e	-10.62
6	6f	-10.47
7	6g	-11.08
8	6h	-10.85
9	6i	-10.95
10	6j	-10.04
11	6k	-10.54
12	6l	-10.88
13	6m	-10.03
14	6n	-10.32

and **6i** exhibited the highest inhibitory potential with a Chemgauss4 score of -10.42 and -10.95, respectively. Different amino acid residues of target enzyme were involved in making binding interactions with the side chains of both compounds **6c** and **6i** (Figures 7 and 8).

Amino acid residues Asp408 and Arg439 were involved in forming two hydrogen bonds with two nitrogen atoms in acetamide and oxadiazole moiety of both compounds **6c** and **6i** as shown in the green dotted line in Figures 7 and 8. In addition, Glu276 and Asp349 were involved in making two π -anion interactions with oxadiazole moiety and adjacent benzene moiety, while the same benzene was involved in making π - π T-shaped with Phe300 (Figures 7 and 8). Apart from hydrogen bonding and electrostatic interaction, hydrophobic interactions were also involved by side chain of compound **6c** with different amino acid residues of Phe157, Leu218, His239, His245, Ala278, and Arg312 target, whereas in case of compound **6i**, two additional hydrophobic interactions were also formed by the addition of methyl group (Figure 8).

2.4.1 | ADME properties of compounds **6a–n**

The ADME properties of molecules were investigated by Med-Chem Designer^[36] and are given in Table 5. It has been reported that the computational methods could be used for the prediction of intestinal drug permeability in rats as in the experimental methods.^[37] The four parameters of Lipinski rule, that is, molecular weight, logP, number of hydrogen-bond acceptors and donors, are thought to be linked with the permeability and solubility, two basic requirements for a drug to have good pharmacokinetic parameters. The properties like polar surface

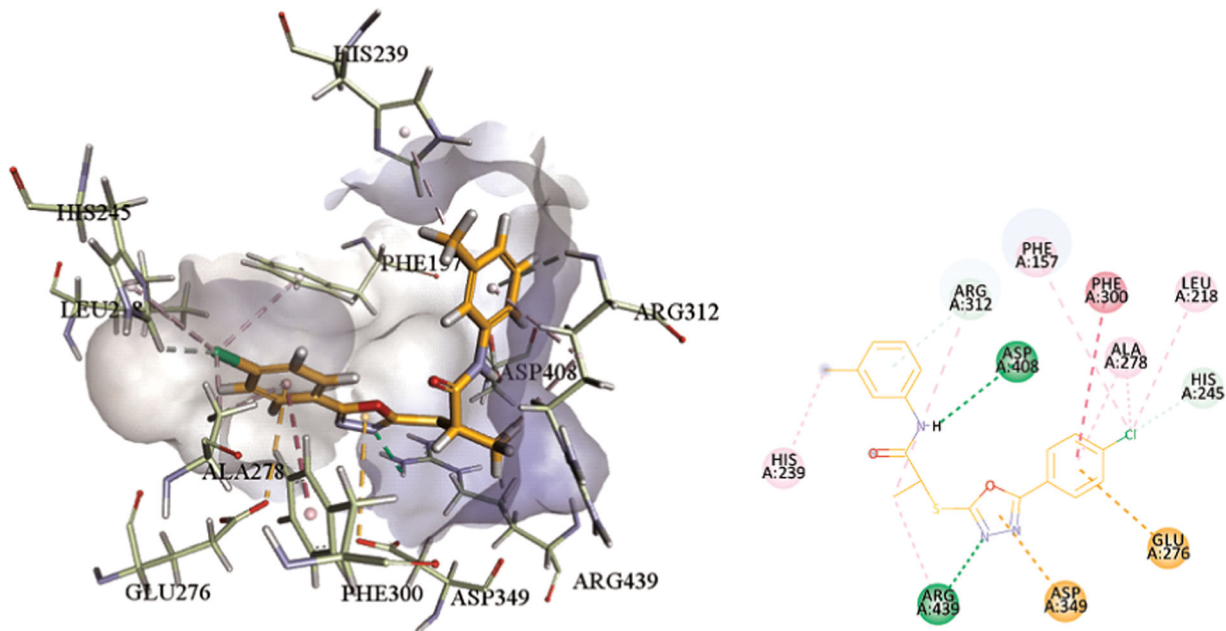


FIGURE 7 Three-dimensional (left) and two-dimensional (right) binding interactions of **6c** within the active site of α -glucosidase. Interacting amino acid residues are shown in light green color, whereas **6c** is shown in golden color. Hydrogen bonding is shown in green dotted form while π - π interaction is shown in pink dotted line, other halogen interactions are shown in cyan color

area and molecular flexibility were considered to have an impact on oral bioavailability. From the table, it can be observed that the compounds having higher logD and logP values and a lower number of hydrogen bonds predict higher bioavailability of drugs.^[37] S+logP and MlogP are octanol-water distribution coefficients and their values are below 5, which indicates that

these molecules have drug-like properties in silico. TPSA is the topological polar surface area. A molecule with a TPSA value exceeding 140 \AA^2 predicts the decreased bioavailability of molecule.^[37] In the present studies, all molecules showed excellent TPSA values between 68.02 and 77.25 \AA^2 . Thus, all these molecules have desirable drug-like TPSA properties.

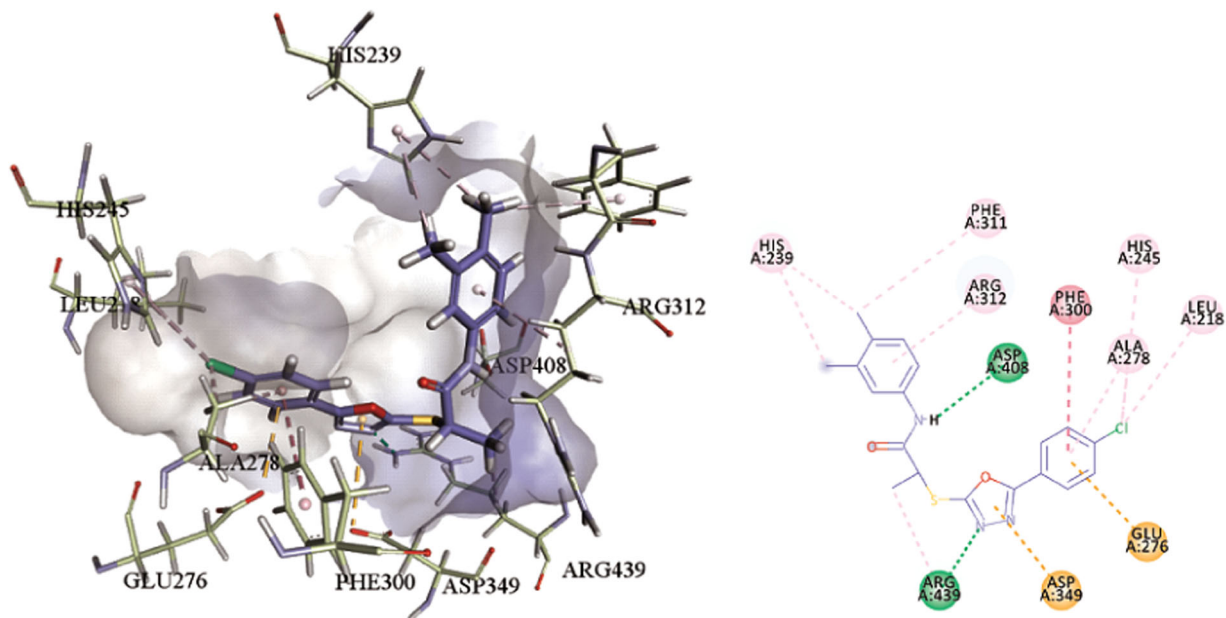


FIGURE 8 Three-dimensional (left) and two-dimensional (right) binding interactions of **6i** within the active site of α -glucosidase. Interacting amino acid residues are shown in light green color, whereas **6i** is shown in golden color. Hydrogen bonding is shown in green dotted form while π - π interaction is shown in pink dotted line, other halogen interactions are shown in cyan color

TABLE 5 Calculated values of ADME (absorption, distribution, metabolism, excretion) properties of compounds

Compound	MlogP	S + logP	S + logD	MWt	MNO	TPSA	HBDH
6a	3.278	3.856	3.856	359.836	5	68.02	1
6b	3.510	4.121	4.121	373.863	5	68.02	1
6c	3.510	4.170	4.170	373.863	5	68.02	1
6d	3.510	4.250	4.250	373.863	5	68.02	1
6e	3.738	4.437	4.437	387.890	5	68.02	1
6f	3.738	4.540	4.540	387.890	5	68.02	1
6g	3.738	4.508	4.508	387.890	5	68.02	1
6h	3.738	4.421	4.421	387.890	5	68.02	1
6i	3.738	4.552	4.552	387.890	5	68.02	1
6j	3.738	4.560	4.560	387.890	5	68.02	1
6k	3.738	4.503	4.502	387.890	5	68.02	1
6l	3.738	4.655	4.655	387.890	5	68.02	1
6m	3.745	4.511	4.511	403.890	6	77.25	1
6n	3.234	4.319	4.319	403.890	6	77.25	1

Note: S + logP and MlogP are octanol-water distribution coefficients (<5.0). S + logD is pH-dependent octanol-water distribution coefficient. HBDH indicates number of hydrogen-bond donors (<5). MNO value indicates the total number of hydrogen-bond acceptor (sum of N and O atoms; <10). MWt is molecular weight (180–480 Da). TPSA is the topological polar surface area expressed in square angstroms (<140 Å²).

3 | CONCLUSIONS

The targeted new *N*-aryl/aralkyl derivatives (**6a–n**) of 2-methyl-2-[5-(4-chlorophenyl)-1,3,4-oxadiazole-2ylthiol]acetamides were synthesized and characterized by spectroscopic methods. Compounds **6a**, **6c–e**, **6g**, and **6i** were found as potent inhibitors of α -glucosidase with IC₅₀ values of 81.72 ± 1.18, 52.73 ± 1.16, 62.62 ± 1.15, 56.34 ± 1.17, 86.35 ± 1.17, 52.63 ± 1.16 μ M, respectively. Molecular docking and ADME studies supported the mode of binding interactions and drug-like properties of the active molecules.

4 | EXPERIMENTAL

4.1 | Chemistry

4.1.1 | General

All the chemicals and solvents of analytical grade were purchased from a local supplier of Sigma-Aldrich and Alfa Aesar. Melting points were measured by Gallenkamp electrothermal apparatus. The purity of the synthesized compounds was confirmed by using silica-coated thin-layer chromatography (TLC) plates F₂₅₆ 20 × 20 cm. ¹H-NMR spectra were recorded on the 400 MHz Bruker spectrometer while ¹³C-NMR spectra were scanned at 100 MHz on the same instrument. The chemical shift values δ were presented on ppm scale using tetramethylsilane as internal standard. Infrared (IR) spectra were recorded as KBr pallets on a Jasco-320-A spectrophotometer. EI-MS and HR-EI-MS spectra were measured on a JMS-HX-110 spectrometer.

The InChI codes of the investigated compounds together with some biological activity data are provided as Supporting Information.

4.1.2 | Synthesis of ethyl 4-chlorobenzoate (1)

4-Chlorobenzoic acid (**a**, 0.03 M; 6.0 g) was dissolved in 50 ml of absolute ethanol with further addition of 5 ml of conc. H₂SO₄ in 250 ml round-bottom. The reaction mixture was refluxed for 2–3 hr. The progress and finally the completion of reaction were monitored by TLC. After completion, the reaction mixture was poured into a separating funnel containing 50 ml of distilled water and was extracted with diethyl ether. The organic layer was condensed under vacuum to get transparent ester **1**.

Colorless oil; yield: 71%; B.P. 237–239°C; IR (KBr): ν = 2,928, 1,755, 1,597 cm⁻¹; ¹H-NMR (500 MHz, CDCl₃): δ = 1.20 (t, *J* = 6.5 Hz, 3H, CH₃–CH₂–O), 4.40 (q, *J* = 6.5 Hz, 2H, O–CH₂–CH₃), Ar-H 7.48 (d, *J* = 8.0 Hz, 2H), and 7.91 (d, *J* = 8.0 Hz, 2H); ¹³C-NMR (125 MHz, CDCl₃): δ = 21.0 (CH₃), 63.0 (CH₂), Ar-C [128.0 (CH), 128.0 (CH), 131.4 (CH), 131.4 (CH), 137.1 (C), and 134.1 (C)], and 166.0 (C=O); HR-EI-MS *m/z*: 184.0291 [M]⁺ calculated for C₉H₉ClO₂; 184.0281.

4.1.3 | Synthesis of 4-chlorobenzohydrazide (2)

Ethyl 4-chlorobenzoate (**1**, 0.02 M; 6.0 ml) and 30 ml of methanol were placed in a 100-ml round-bottom flask. Ten milliliters of 0.02 M hydrazine hydrate (80%) was added to the reaction mixture and was refluxed for 4–5 hr. The solvent was distilled off and cold distilled water was added with shaking till the appearance of precipitates of 4-chlorobenzohydrazide (**2**) which was then filtered, washed with distilled water and dried.

Yellow crystals; yield 76%; M.P.: 162–165°C; IR (KBr): ν = 3,410, 3,305, 2,925, 1,688, 1,520 cm⁻¹; ¹H-NMR (500 MHz, CDCl₃): δ 4.06 (s, –NH₂, 1H), Ar-H, 7.55 (d, 2H, CH, *J* = 8.5 Hz), 7.80 (d, 2H, CH, *J* = 8.5 Hz), 8.90 (s, –NH, 1H); ¹³C-NMR (125 MHz, CDCl₃): δ Ar-C [127.3 (CH), 128.0 (CH), 129.8 (CH), 129.9 (CH), 133.1 (C), 136.3 (C)],

164.9 (C=O); HR-EI-MS (m/z): 170.0247 $[M]^+$ calculated for $C_7H_7ClN_2O$; 170.0237.

4.1.4 | Synthesis of 5-(4-chlorophenyl)-1,3,4-oxadiazole-2-thiol (3)

4-Chlorobenzohydrazide (**2**; 0.025 M; 4.0 g) was dissolved in 30 ml of absolute ethanol and placed in a 100-ml round-bottom flask. Carbon disulfide (0.025 M; 6.5 ml) was added to the flask followed by the addition of potassium hydroxide (0.03 M; 2.0 g). The mixture was refluxed for 6–7 hr with stirring. After completion of the reaction, the mixture was diluted with 30 ml of distilled water and acidified with dilute HCl to pH 2.0. The precipitates of 5-(4-chlorophenyl)-1,3,4-oxadiazole-2-thiol (**3**) were filtered, washed with distilled water, and crystallized from ethanol.

Amorphous pink solid; yield 66%; M.P.: 135–138°C; IR (KBr): $\nu = 3,417, 3,325, 2,910, 1,520 \text{ cm}^{-1}$. $^1\text{H-NMR}$ (500 MHz, CDCl_3): $\delta = \text{Ar-H}, 7.45 \text{ (d, } J = 8.5 \text{ Hz, 1H)}, 7.80 \text{ (d, } J = 8.5 \text{ Hz, 2H, H-2'',6''), and } 12.31 \text{ (s, 1H, -SH)}$; $^{13}\text{C-NMR}$ (125 MHz, CDCl_3): $\delta = \text{Ar-C [126.3 (CH), 127.0 (CH), 128.8 (CH), 128.9 (CH), 133.1 (C), 134.3 (C), 145.1 (C), and } 159.8 \text{ (C)]}$; HR-EI-MS (m/z): 211.9811 $[M]^+$ calculated for $C_8H_5ClN_2OS$; 211.9801.

4.1.5 | Synthesis of compounds (5a–n)

The calculated amount of aryl/aralkyl amines (**4a–n**, 11.0 mM each) was added to 10 ml of distilled water in an iodine flask containing 5% Na_2CO_3 solution to adjust the pH 9–10. The reaction mixture was stirred for 10 min and then 2-bromopropionyl bromide (1.0 ml, 11.0 mM) was poured into the reaction mixture drop-wise in 2–5 min with constant stirring. The flask was shaken vigorously until the precipitates formed and the room temperature was achieved. The precipitates were further stirred for 45 min. The reaction progress was monitored by TLC (*n*-hexane/ethylacetate; 7:3). The final products were filtered, washed with distilled water, dried to get the respective *N*-aralkyl/aryl-substituted-2-bromopropionamides (**5a–n**).

4.1.6 | Synthesis of compounds (6a–n)

Compound **3** (0.002 g, 0.1 mM) was dissolved in *N,N*-dimethylformamide (DMF, 10 ml) in a 50-ml round-bottom flask followed by the addition of sodium hydride (0.002 g, 0.1 mM). The mixture was stirred for 30 min at room temperature and then electrophiles (**5a–n** each, respectively) were added slowly with further stirring for 2–3 hr. Distilled water was added to the flask and the products were recovered by filtration or solvent extraction according to the product nature.

2-[[5-(4-Chlorophenyl)-1,3,4-oxadiazol-2-yl]thio]-*N*-phenylpropanamide (**6a**)

Yield: 78%; M.P.: 135–136°C; IR (KBr): $\nu = 3,020, 2,920, 1,696, 1,597, \text{ and } 1,535 \text{ cm}^{-1}$; $^1\text{H-NMR}$ (500 MHz, CDCl_3): $\delta = 1.73 \text{ (d, } J = 7.0 \text{ Hz,}$

3H, H-3), 4.52 (q, $J = 7.5 \text{ Hz, 1H, H-2}$), Ar-H 7.07–7.11 (m, 5H, CH), 7.48 (d, $J = 8.5 \text{ Hz, 2H, H-3'',5''}$), 7.91 (d, $J = 8.5 \text{ Hz, 2H, H-2'',6''}$), 9.21 (s, 1H, NH); $^{13}\text{C-NMR}$ (125 MHz, CDCl_3): $\delta = 16.8 \text{ (C-3)}, 44.6 \text{ (C-2)}, \text{Ar-C [119.8 (C-2''), 121.5 (C-2'',6''), 126.5 (C-3'',5''), 129.6 (C-5''), 134.7 (C-6''), 136.2 (C-3''), 137.7 (C-4''), 138.4 (C-1''), 138.4 (C-1''), 141.1 (C-4''), 165.1 (C-5), 165.3 (C-2), and } 168.2 \text{ (C-1)]}$; HR-EI-MS (m/z): 359.0497 $[M]^+$ calculated for $C_{17}H_{14}ClN_3O_2Cl$; 359.0485.

2-[[5-(4-Chlorophenyl)-1,3,4-oxadiazol-2-yl]thio]-*N*-(2-methylphenyl)propanamide (**6b**)

Yield: 69%; M.P.: 131–133°C; IR (KBr): $\nu = 3,029, 2,920, 1,701, 1,590, \text{ and } 1,530 \text{ cm}^{-1}$; $^1\text{H-NMR}$ (500 MHz, CDCl_3): $\delta = 1.45 \text{ (d, } J = 7.0 \text{ Hz, 3H, H-3)}, 1.77 \text{ (s, 3H, Ar-CH}_3\text{)}, 4.35 \text{ (q, } J = 7.0 \text{ Hz, 1H, H-2)}, \text{Ar-H } 7.16\text{--}7.21 \text{ (m, 4H)}, 7.40 \text{ (d, } J = 8.5 \text{ Hz, 2H, H-3'',5''), 7.88 \text{ (d, } J = 8.5 \text{ Hz, 2H, H-2'',6''), and } 8.55 \text{ (s, 1H, NH)}$; $^{13}\text{C-NMR}$ (125 MHz, CDCl_3): $\delta = 16.0 \text{ (C-3)}, 21.1 \text{ (CH}_3\text{)}, 42.8 \text{ (C-2)}, \text{Ar-C [120.8 (C-2''), 121.9 (C-2'',6''), 125.0 (C-3'',5''), 129.6 (C-5''), 132.5 (C-6''), 136.2 (C-3''), 136.3 (C-4''), 136.4 (C-1''), 138.4 (C-1''), 141.1 (C-4''), 142.1 (C-5), 149.3 (C-2), and } 160.2 \text{ (C-1)]}$; HR-EI-MS (m/z): 373.0655 $[M]^+$ calculated for $C_{18}H_{16}ClN_3O_2Cl$; 373.0642.

2-[[5-(4-Chlorophenyl)-1,3,4-oxadiazol-2-yl]thio]-*N*-(3-methylphenyl)propanamide (**6c**)

Yield: 70%; M.P.: 132–134°C; IR (KBr): $\nu = 3,032, 2,940, 1,690, 1,605, \text{ and } 1,550 \text{ cm}^{-1}$; $^1\text{H-NMR}$ (500 MHz, CDCl_3): $\delta = 1.49 \text{ (d, } J = 7.0 \text{ Hz, 3H, H-3)}, 1.74 \text{ (s, 3H, CH}_3\text{)}, 4.45 \text{ (q, } J = 7.0 \text{ Hz, 1H, H-2)}, \text{Ar-H } 7.42 \text{ (s, 1H, H-2''), 7.55 \text{ (d, } J = 8.0 \text{ Hz, 1H, H-4''), 7.60 \text{ (dd, } J = 8.5, 7.0 \text{ Hz, 1H, H-5''), 7.62 \text{ (d, } J = 8.0 \text{ Hz, 1H, H-6''), 7.72 \text{ (d, } J = 8.5 \text{ Hz, 2H, H-3',5')}, 7.96 \text{ (d, } J = 8.5 \text{ Hz, 2H, H-2',6')}, \text{ and } 9.96 \text{ (s, 1H, NH)}$; $^{13}\text{C-NMR}$ (125 MHz, CDCl_3): $\delta = 19.8 \text{ (C-3)}, 21.1 \text{ (CH}_3\text{)}, 39.8 \text{ (C-2)}, \text{Ar-C [117.8 (C-2''), 120.1 (C-2'',6''), 127.0 (C-3'',5''), 128.7 (C-5''), 129.3 (C-6''), 130.0 (C-3''), 132.4 (C-4''), 135.3 (C-1''), 136.9 (C-1''), 140.7 (C-4''), 142.3 (C-5), 147.3 (C-2), and } 166.0 \text{ (C-1)]}$; HR-EI-MS (m/z): 373.0658 $[M]^+$ calculated for $C_{18}H_{16}ClN_3O_2Cl$; 373.0642.

2-[[5-(4-Chlorophenyl)-1,3,4-oxadiazol-2-yl]thio]-*N*-(4-methylphenyl)propanamide (**6d**)

Yield: 79%; M.P.: 135–137°C; IR (KBr): $\nu = 3,020, 2,920, 1,696, 1,597, \text{ and } 1,535 \text{ cm}^{-1}$; $^1\text{H-NMR}$ (500 MHz, CDCl_3): $\delta = 1.38 \text{ (d, } J = 7.0 \text{ Hz, 3H, H-3)}, 2.50 \text{ (s, 3H, CH}_3\text{)}, 4.38 \text{ (q, } J = 7.0 \text{ Hz, 1H, H-2)}, \text{Ar-H } 7.42 \text{ (d, } J = 8.5 \text{ Hz, 2H, H-2'',6''), 7.55 \text{ (d, } J = 8.5 \text{ Hz, 2H, H-3'',5''), 7.61 \text{ (d, } J = 8.5 \text{ Hz, 2H, H-3'',5''), 7.70 \text{ (d, } J = 8.5 \text{ Hz, 2H, H-2'',6''), 9.25 \text{ (s, 1H, NH)}$; $^{13}\text{C-NMR}$ (125 MHz, CDCl_3): $\delta = 20.8 \text{ (C-3)}, 21.9 \text{ (CH}_3\text{)}, 37.6 \text{ (C-2)}, \text{Ar-C [119.3 (C-2''), 120.1 (C-2'',6''), 126.0 (C-3'',5''), 129.9 (C-5''), 130.3 (C-6''), 130.7 (C-3''), 131.4 (C-4''), 134.3 (C-1''), 137.9 (C-1''), 142.1 (C-4''), 142.8 (C-5), 149.3 (C-2), and } 166.1 \text{ (C-1)]}$; HR-EI-MS (m/z): 373.0658 $[M]^+$ calculated for $C_{18}H_{16}ClN_3O_2Cl$; 373.0642.

2-[[5-(4-Chlorophenyl)-1,3,4-oxadiazol-2-yl]thio]-*N*-(2,3-dimethylphenyl)propanamide (**6e**)

Yield: 73%; M.P.: 127–139°C; IR (KBr): $\nu = 3,029, 2,918, 1,688, 1,591, \text{ and } 1,529 \text{ cm}^{-1}$; $^1\text{H-NMR}$ (500 MHz, CDCl_3): $\delta = 1.39 \text{ (d, } J = 7.0 \text{ Hz,}$

3H, H-3), 1.78 (s, 3H, CH₃), 2.10 (s, 3H, CH₃), 4.45 (q, *J* = 7.0 Hz, 1H, H-2), Ar-H 7.42–7.46 (m, 1H, CH), 7.45 (d, *J* = 8.5 Hz, 2H, H-3",5"), and 7.68 (d, *J* = 8.5 Hz, 2H, H-2",6"); ¹³C-NMR (125 MHz, CDCl₃): δ = 21.7 (C-3'), 23.1 (CH₃), 25.1 (CH₃), 34.6 (C-2), Ar-C [117.3 (C-2''), 120.1 (C-2",6"), 128.0 (C-3",5"), 128.9 (C-5'''), 130.5 (C-6''), 130.9 (C-3'''), 133.4 (C-4''), 138.3 (C-1'''), 139.9 (C-1"), 142.7 (C-4"), 142.8 (C-5), 149.3 (C-2), and 168.0 (C-1)]; HR-EI-MS (*m/z*): 387.0812 [M]⁺ calculated for C₁₉H₁₈SN₃O₂Cl; 387.0798.

2-[[5-(4-Chlorophenyl)-1,3,4-oxadiazol-2-yl]thio]-N-(2,4-dimethylphenyl)propanamide (6f)

Yield: 65%; M.P.: 139–140°C; IR (KBr): *v* = 3,045, 2,945, 1,710, 1,605, and 1,545 cm⁻¹; ¹H-NMR (500 MHz, CDCl₃): δ = 1.40 (d, *J* = 7.0 Hz, 3H, H-3), 1.69 (s, 3H, CH₃), 1.70 (s, 3H, CH₃), 4.40 (q, *J* = 7.0 Hz, 1H, H-2), Ar-H 7.35 (s, 1H, H-3''), 7.42 (d, *J* = 8.5 Hz, 1H, H-5''), 7.47 (d, *J* = 8.5 Hz, 1H, H-6'''), 7.58 (d, *J* = 8.5 Hz, 2H, H-3",5"), and 7.68 (d, *J* = 8.5 Hz, 2H, H-2",6"); ¹³C-NMR (125 MHz, CDCl₃): δ = 23.1 (C-3'), 23.5 (CH₃), 25.7 (CH₃), 34.0 (C-2'), Ar-C [118.5 (C-2''), 121.7 (C-2",6''), 126.0 (C-3",5"), 127.9 (C-5'''), 129.5 (C-6''), 132.5 (C-3'''), 133.9 (C-4''), 134.3 (C-1'''), 138.1 (C-1"), 142.7 (C-4"), 142.8 (C-5), 144.3 (C-2), and 162.0 (C-1)]; HR-EI-MS (*m/z*): 387.0812 [M]⁺ calculated for C₁₉H₁₈SN₃O₂Cl; 387.0798.

2-[[5-(4-Chlorophenyl)-1,3,4-oxadiazol-2-yl]thio]-N-(2,5-dimethylphenyl)propanamide (6g)

Yield: 71%; M.P.: 157–159°C; IR (KBr): *v* = 3,020, 2,920, 1,696, 1,597, and 1,535 cm⁻¹; ¹H-NMR (500 MHz, CDCl₃): δ = 1.60 (d, *J* = 7.0 Hz, 3H, H-3'), 1.69 (s, 3H, CH₃), 1.70 (s, 3H, CH₃), 4.42 (q, 1H, H-2', *J* = 7.0 Hz), Ar-H 7.35 (s, 1H, H-6''), 7.41 (d, *J* = 8.5 Hz, 1H, H-3'''), 7.45 (d, *J* = 8.5 Hz, 1H, H-4''), 7.59 (d, *J* = 8.5 Hz, 2H, H-3",5"), and 7.70 (d, *J* = 8.5 Hz, 2H, H-2",6"); ¹³C-NMR (125 MHz, CDCl₃): δ = 20.1 (C-3), 22.5 (CH₃), 25.9 (CH₃), 34.1 (C-2), Ar-C [120.5 (C-2''), 121.1 (C-2",6"), 126.4 (C-3",5"), 127.9 (C-5'''), 129.5 (C-6''), 130.5 (C-3'''), 133.9 (C-4''), 134.3 (C-1'''), 138.1 (C-1"), 142.7 (C-4"), 142.8 (C-5), 144.3 (C-2), and 162.0 (C-1)]; HR-EI-MS (*m/z*): 387.0812 [M]⁺ calculated for C₁₉H₁₈SN₃O₂Cl; 387.0798.

2-[[5-(4-Chlorophenyl)-1,3,4-oxadiazol-2-yl]thio]-N-(2,6-dimethylphenyl)propanamide (6h)

Yield: 70%; M.P.: 140–142°C; IR (KBr): *v* = 3,030, 2,929, 1,692, 1,589, and 1,525 cm⁻¹; ¹H-NMR (500 MHz, CDCl₃): δ = 1.34 (d, *J* = 7.0 Hz, 3H, H-3'), 1.66 (s, 3H, CH₃), 2.19 (s, 3H, CH₃), 4.45 (q, 1H, H-2', *J* = 7.0 Hz), Ar-H 7.42–7.46 (m, 1H, 3CH), 7.49 (d, *J* = 8.5 Hz, 2H, H-3",5"), and 7.60 (d, *J* = 8.5 Hz, 2H, H-2",6"); ¹³C-NMR (125 MHz, CDCl₃): δ = 21.7 (C-3'), 23.1 (CH₃), 25.1 (CH₃), 34.6 (C-2), Ar-C [117.3 (C-2''), 120.1 (C-2",6"), 128.0 (C-3",5"), 128.9 (C-5'''), 130.5 (C-6''), 130.9 (C-3'''), 133.4 (C-4''), 138.3 (C-1'''), 139.9 (C-1"), 142.7 (C-4"), 142.8 (C-5), 149.3 (C-2), and 168.0 (C-1)]; HR-EI-MS [M]⁺ (*m/z*): 387.0812 calculated for C₁₉H₁₈SN₃O₂Cl; 387.0798.

2-[[5-(4-Chlorophenyl)-1,3,4-oxadiazol-2-yl]thio]-N-(3,4-dimethylphenyl)propanamide (6i)

Yield: 70%; M.P.: 138–140°C; IR (KBr): *v* = 3,035, 2,925, 1,696, 1,590, and 1,535 cm⁻¹; ¹H-NMR (500 MHz, CDCl₃): δ = 1.45 (d, *J* = 7.0 Hz, 3H, H-3), 1.68 (s, 3H, CH₃), 1.72 (s, 3H, CH₃), 4.39 (q, *J* = 7.5 Hz, 1H, H-2'), Ar-H 7.55 (s, 1H, H-2''), 7.67 (d, *J* = 8.5 Hz, 1H, H-5''), 7.72 (d, *J* = 8.5 Hz, 1H, H-6''), 7.88 (d, *J* = 8.5 Hz, 2H, H-3",5"), and 7.70 (d, *J* = 8.5 Hz, 2H, H-2",6"); ¹³C-NMR (125 MHz, CDCl₃): δ = 21.1 (C-3'), 22.1 (CH₃), 23.9 (CH₃), 34.7 (C-2), Ar-C [120.5 (C-2''), 121.1 (C-2",6"), 126.4 (C-3",5"), 127.9 (C-5'''), 129.5 (C-6''), 132.5 (C-3'''), 133.4 (C-4''), 134.5 (C-1'''), 138.1 (C-1"), 142.7 (C-4"), 147.8 (C-5), 149.3 (C-2), and 160.0 (C-1)]; HR-EI-MS (*m/z*): 387.0812 [M]⁺ calculated for C₁₉H₁₈SN₃O₂Cl; 387.0798.

2-[[5-(4-Chlorophenyl)-1,3,4-oxadiazol-2-yl]thio]-N-(3,5-dimethylphenyl)propanamide (6j)

Yield: 75%; M.P.: 133–135°C; IR (KBr): *v* = 3,025, 2,929, 1,696, 1,588, and 1,545 cm⁻¹; ¹H-NMR (500 MHz, CDCl₃): δ = 1.76 (d, *J* = 7.0 Hz, 3H, H-3), 1.77 (s, 3H, CH₃), 2.13 (s, 3H, CH₃), 4.45 (q, *J* = 7.0 Hz, 1H, H-2'), Ar-H 7.21 (s, 1H, H-2''), 7.29 (s, 1H, H-4''), 7.31 (s, 1H, H-6''), 7.42 (d, *J* = 8.5 Hz, 2H, H-3",5"), 7.60 (d, *J* = 8.5 Hz, 2H, H-2",6"), and 8.75 (s, 1H, NH); ¹³C-NMR (125 MHz, CDCl₃): δ = 19.7 (C-3), 21.1 (CH₃), 23.1 (CH₃), 33.6 (C-2), Ar-C [119.7 (C-2''), 120.1 (C-2",6"), 127.0 (C-3",5"), 128.9 (C-5'''), 130.5 (C-6''), 130.9 (C-3'''), 133.4 (C-4''), 138.3 (C-1'''), 139.9 (C-1"), 141.7 (C-4"), 142.8 (C-5), 149.3 (C-2), and 160.0 (C-1)]; HR-EI-MS (*m/z*): 387.0812 [M]⁺ calculated for C₁₉H₁₈SN₃O₂Cl; 387.0798.

2-[[5-(4-Chlorophenyl)-1,3,4-oxadiazol-2-yl]thio]-N-(2-ethylphenyl)propanamide (6k)

Yield: 71%; M.P.: 133–135°C; IR (KBr): *v* = 3,029, 2,920, 1,701, 1,590, and 1,540 cm⁻¹; ¹H-NMR (500 MHz, CDCl₃): δ = 1.16 (t, *J* = 6.5 Hz, 3H, CH₃-CH₂), 1.39 (d, *J* = 7.0 Hz, 3H, H-3'), 2.60 (q, *J* = 6.5 Hz, 2H, CH₂-CH₃), 4.35 (q, *J* = 7.0 Hz, 1H, H-2'), Ar-H 7.21–7.26 (m, 4H, CH), 7.48 (d, *J* = 8.5 Hz, 2H, H-3",5"), 7.93 (d, *J* = 8.5 Hz, 2H, H-2",6"), and 8.75 (s, 1H, NH); ¹³C-NMR (125 MHz, CDCl₃): δ = 14.1 (C-3), 17.0 (CH₃), 24.5 (CH₂), 44.5 (C-2), Ar-C [121.5 (C-2''), 123.4 (C-2",6"), 126.5 (C-3",5"), 128.7 (C-5'''), 129.6 (C-6''), 134.8 (C-3'''), 135.3 (C-4''), 138.3 (C-1'''), 139.9 (C-1"), 149.7 (C-4"), 165.0 (C-5), 165.4 (C-2), and 168.7 (C-1)]; HR-EI-MS (*m/z*): 387.0812 [M]⁺ calculated for C₁₉H₁₈SN₃O₂Cl; 387.0798.

2-[[5-(4-Chlorophenyl)-1,3,4-oxadiazol-2-yl]thio]-N-(4-ethylphenyl)propanamide (6l)

Yield: 73%; M.P.: 138–141°C; IR (KBr): *v* = 3,025, 2,920, 1,696, 1,605, and 1,532 cm⁻¹; ¹H-NMR (500 MHz, CDCl₃): δ = 1.28 (t, *J* = 6.4 Hz, 3H, CH₃-CH₂), 1.40 (d, *J* = 7.0 Hz, 3H, H-3'), 2.19 (q, *J* = 6.4 Hz, 2H, CH₂-CH₃), 4.21 (q, *J* = 7.0 Hz, 1H, H-2'), Ar-H 7.10 (d, *J* = 8.5 Hz, 2H, H-2",6''), 7.18 (d, *J* = 8.5 Hz, 2H, H-3",5''), 7.48 (d, *J* = 8.5 Hz, 2H, H-3",5"), 7.93 (d, *J* = 8.5 Hz, 2H, H-2",6"), and 8.75 (s, 1H, NH); ¹³C-NMR (125 MHz, CDCl₃): δ = 14.1 (CH₃), 17.0 (C-3'), 24.5 (CH₂), 44.5 (C-2), Ar-C [121.5 (C-2''), 123.4 (C-2",6"), 126.5 (C-3",5"), 128.7 (C-5'''), 129.6 (C-6''), 134.8 (C-3'''), 135.3 (C-4''), 138.3 (C-1'''), 139.9

(C-1''), 149.7 (C-4''), 165.0 (C-5), 165.4 (C-2), and 168.7 (C-1)]; HR-EI-MS (*m/z*): 387.0812 [*M*]⁺ calculated for C₁₉H₁₈SN₃O₂Cl; 387.0798.

2-[[5-(4-Chlorophenyl)-1,3,4-oxadiazol-2-yl]thio]-N-(2-ethoxyphenyl)propanamide (6m)

Yield: 65%; M.P.: 140–142°C; IR (KBr): $\nu = 3,029, 2,929, 1,710, 1,592, \text{ and } 1,529 \text{ cm}^{-1}$; ¹H-NMR (500 MHz, CDCl₃): $\delta = 1.37$ (t, *J* = 6.6 Hz, 3H, CH₃-CH₂), 1.72 (d, *J* = 7.5 Hz, 3H, H-3'), 3.99 (q, *J* = 7.0 Hz, 2H, CH₃-CH₂), 4.35 (q, *J* = 7.5 Hz, 1H, H-2), Ar-H 7.16–7.19 (m, 4H, CH), 6.81 (d, *J* = 8.5 Hz, 2H, H-3'',5''), 7.92 (d, *J* = 8.5 Hz, 2H, H-2'',6''), and 8.75 (s, 1H, NH); ¹³C-NMR (125 MHz, CDCl₃): $\delta = 14.8$ (CH₃), 16.9 (C-3'), 63.6 (CH₂), 44.7 (C-2'), Ar-C [113.2 (C-2''), 121.5 (C-2'',6''), 121.6 (C-5''), 125.5 (C-3'',5''), 128.0 (C-6''), 129.5 (C-3''), 130.7 (C-4''), 138.4 (C-1''), 155.8 (C-1''), 165.1 (C-4''), 165.3 (C-5), 165.4 (C-2), and 168.0 (C-1)]; HR-EI-MS (*m/z*): 403.0759 [*M*]⁺ calculated for C₁₉H₁₈SN₃O₃Cl; 403.0747.

2-[[5-(4-Chlorophenyl)-1,3,4-oxadiazol-2-yl]thio]-N-(4-ethoxyphenyl)propanamide (6n)

Yield: 77%; M.P.: 133–134°C; IR (KBr): $\nu = 3,035, 2,920, 1,690, 1,590, \text{ and } 1,545 \text{ cm}^{-1}$; ¹H-NMR (500 MHz, CDCl₃): $\delta = 1.35$ (t, *J* = 6.6 Hz; 3H, CH₃-CH₂-O), 1.39 (d, *J* = 7.0 Hz, 3H, H-3'), 3.45 (q, *J* = 6.6 Hz, 2H, O-CH₂-CH₃), 4.35 (q, *J* = 7.0 Hz, 1H, H-2), Ar-H 7.12 (d, *J* = 8.5 Hz, 2H, H-2'',6''), 7.21 (d, *J* = 8.5 Hz, 2H, H-3'',5''), 7.54 (d, *J* = 8.5 Hz, 1H, H-3'',5''), 7.88 (d, *J* = 8.5 Hz, 2H, H-2'',6''), and 8.75 (s, 1H, NH); ¹³C-NMR (125 MHz, CDCl₃): $\delta = 14.8$ (CH₃), 16.9 (C-3), 59.3 (CH₂), 44.7 (C-2), Ar-C [113.2 (C-2''), 121.5 (C-2'',6''), 121.6 (C-5''), 126.7 (C-3'',5''), 129.0 (C-6''), 129.5 (C-3''), 131.7 (C-4''), 136.4 (C-1''), 142.3 (C-1''), 160.1 (C-4''), 161.3 (C-5), 165.4 (C-2), and 168.7 (C-1)]; HR-EI-MS (*m/z*): 403.0759 [*M*]⁺ calculated for C₁₉H₁₈SN₃O₃Cl; 403.0747.

4.2 | α -Glucosidase inhibition assay

Yeast α glucosidase inhibition assay was performed according to the method used by Tariq et al.^[38] Total reaction volume of 100 μ l contained 70 μ l of 50 mM phosphate buffer pH 6.8, 10- μ l (0.5 mM) test compound, followed by the addition of 10 μ l (0.057 units) yeast enzyme (Sigma Inc.). The contents were mixed, preincubated for 10 min at 37°C, and pre-read at 400 nm. The reaction was initiated by the addition of 10 μ l of 0.5 mM substrate (*p*-nitrophenyl- α -D-glucopyranoside). After 25–30 min of incubation at 37°C, absorbance was measured using Synergy HST microplate reader (BioTek). All experiments were carried out in triplicates and the data are presented as mean \pm standard error of the mean. Acarbose was used as positive control. The percentage inhibition of the enzyme was calculated using the following formula.

$$\text{Inhibition (\%)} = \left(\frac{\text{Abs of control} - \text{Abs of comp}}{\text{Abs of control}} \right) \times 100$$

The IC₅₀ values of the active compounds were calculated from the data obtained by measuring inhibitory activities of compounds after their suitable dilutions using Ez-Fit Perella Scientific software.

4.3 | Homology modeling of yeast α -glucosidase

The homology model of α -glucosidase from *S. cerevisiae* was built because to date no crystal structure of α -glucosidase has been reported in PDB. The amino acid sequence of α -glucosidase was retrieved from using UniProt ID P53341 and aligned with the best selected template of isomaltase from *S. cerevisiae* (PDB ID: 3A4A).^[39] Sequence alignment was carried using "zAlign sequence to template" tool in Discovery Studio Client vs 16.1 program and homology modeling was also performed out using built in Modeler v. 9.15 in DS software.^[40] The best homology model was selected on the basis of the DOPE score while validation and assessment were conducted via Ramachandran plot using RAMPAGE.^[41]

4.4 | Molecular docking studies

Molecular docking calculations were performed using FRED tool in Open Eye software.^[42,43] All the compounds were first drawn in Chemdraw Professionals ver. 15.1^[44] and then were imported into Discovery Studio for 3D structure generation and energy minimization. OMEGA 2.5 tool of Open Eye software was used for generation of conformers of compounds.^[45,46] Active site was selected on the basis of modeled cocrystal ligand α -glucose. Before molecular docking studies, docking protocol was optimized for cocrystal ligand and then final docking was carried out for all the compounds as well as the reference compound for comparison. During docking calculations, 20 different poses were generated and sorted out based on the lowest Chemgauss4 score. Binding orientations were also visualized using Discovery Studio software.^[39]

ACKNOWLEDGMENT

We are thankful to Open Eye Scientific for providing free academic license of Open Eye Suite.

ORCID

Naheed Riaz  <http://orcid.org/0000-0002-6890-882X>

REFERENCES

- [1] C. S. de Oliveira, B. F. Lira, J. M. Barbosa-Filho, J. G. F. Lorenzo, P. F. de Athayde-Filho, *Molecules* **2012**, *17*, 10192.
- [2] K. D. Patel, S. M. Prajapati, S. N. Panchal, H. D. Patel, *Syn. Commun.* **2014**, *44*, 1859.
- [3] I. Hirao, Y. Kato, T. Hirota, *Bull. Chem. Soc. Jpn.* **1971**, *44*, 1923.
- [4] R. Schlexer, P. C. Thieme, *Tetrahedron* **1988**, *44*, 3289.
- [5] E. Serrao, S. Odde, K. Ramkumar, N. Neamati, *Retrovirology* **2009**, *6*, 25.

- [6] S. Vardan, H. Smulyan, S. Mookherjee, R. Eich, *Clin. Pharmacol. Ther.* **1983**, *34*, 290.
- [7] A. Adhikari, B. Kalluraya, K. V. Sujith, K. Gouthamchandra, R. Jairam, R. Mahmood, R. Sankolli, *Eur. J. Med. Chem.* **2012**, *55*, 467.
- [8] R. Chawla, A. Arora, M. K. Parameswaran, P. C. Sharma, S. Michael, T. K. Ravi, *Synthesis* **2010**, *18*, 123.
- [9] K. K. Jha, A. Samad, Y. Kumar, M. Shaharyar, R. L. Khosa, J. Jain, V. Kumar, P. Singh, *Eur. J. Med. Chem.* **2010**, *45*, 4963.
- [10] A. Husain, A. Ahmad, M. M. Alam, M. Ajmal, P. Ahuja, *Eur. J. Med. Chem.* **2009**, *44*, 3798.
- [11] M. S. Yar, A. A. Siddiqui, M. Ashraf Ali, *J. Chin. Chem. Soc.* **2007**, *54*, 5.
- [12] M. A. Ali, M. Shaharyar, *Bioorg. Med. Chem. Lett.* **2007**, *17*, 3314.
- [13] Y. Ünver, H. Gökce, E. Bektaş, F. Çelik, I. Değirmencioglu, *Can. J. Chem.* **2018**, *96*, 1047.
- [14] Au Rehman, N. Ahtzaz, M. A. Abbasi, S. Z. Siddiqui, S. Saleem, S. Manzoor, J. Iqbal, N. A. Virk, T. A. Chohan, S. Shah, *Trop. J. Pharm. Res.* **2018**, *17*, 1145.
- [15] P. P. Roy, S. Bajaj, T. K. Maity, J. Singh, *Receptor* **2017**, *1*, 15.
- [16] J. Sun, H. Zhu, Z.-M. Yang, H.-L. Zhu, *Eur. J. Med. Chem.* **2013**, *60*, 23.
- [17] H.-Z. Zhang, S. Kasibhatla, J. Kuemmerle, W. Kemnitzer, K. Ollis-Mason, L. Qiu, C. Crogan-Grundy, B. Tseng, J. Drewe, S. X. Cai, *J. Med. Chem.* **2005**, *48*, 5215.
- [18] M. M. Gamal el-Din, M. I. El-Gamal, M. S. Abdel-Maksoud, K. H. Yoo, C. H. Oh, *Eur. J. Med. Chem.* **2015**, *90*, 45.
- [19] W. A. El-Sayed, F. A. El-Essawy, O. M. Ali, B. S. Nasr, M. M. Abdalla, A. A. H. Abdel-Rahman, *Z. Naturforsch. C* **2009**, *64c*, 773.
- [20] P.-Y. Wang, W.-B. Shao, H.-T. Xue, H.-S. Fang, J. Zhou, Z.-B. Wu, B.-A. Song, S. Yang, *Res. Chem. Intermed.* **2017**, *43*, 6115.
- [21] A. Zarghi, Z. Hajimahdi, S. Mohebbi, H. Rashidi, S. Mozaffari, S. Sarraf, M. Faizi, S. A. Tabatabaee, A. Shafiee, *Chem. Pharm. Bull.* **2008**, *56*, 509.
- [22] M. A. Bhat, N. Siddiqui, S. A. Khan, *Acta Pol. Pharm. Drug Res.* **2008**, *65*, 235.
- [23] K. M. Khan, M. Ashraf, I. Ahmad, S. A. Ejaz, *Pak. J. Pharm. Sci.* **2013**, *26*, 345.
- [24] S. Valente, D. Trisciuglio, T. De Luca, A. Nebbioso, D. Labella, A. Lenoci, C. Bigogno, G. Dondio, M. Miceli, G. Brosch, D. Del-Bufalo, L. Altucci, A. Mai, *J. Med. Chem.* **2014**, *57*, 6259.
- [25] D. Q. Qi, C. M. Yu, J. Z. You, G. H. Yang, X. J. Wang, Y. P. Zhang, *J. Mol. Struct.* **2015**, *1100*, 421.
- [26] H. Lai, D. Dou, S. Aravapalli, T. Teramoto, G. H. Lushington, T. M. Mwanja, K. R. Alliston, D. M. Eichhorn, R. Padmanabhan, W. C. Groutas, *Bioorg. Med. Chem.* **2013**, *21*, 102.
- [27] S. Nazreen, M. S. Alam, H. Hamid, M. S. Yar, S. Shafi, A. Dhulap, P. Alam, M. A. Q. Pasha, S. Bano, M. M. Alam, S. Haider, Y. Ali, C. Kharbanda, K. K. Pillai, *Eur. J. Med. Chem.* **2014**, *87*, 175.
- [28] R. Bhutani, D. P. Pathak, G. Kapoor, A. Husain, M. A. Iqbal, *Bioorg. Chem.* **2019**, *83*, 6.
- [29] R. Nirogi, A. R. Mohammed, A. K. Shinde, S. R. Gagginapally, D. M. Kancharla, V. R. Middekadi, N. Bogaraju, S. R. Ravella, P. Singh, S. R. Birangal, R. Subramanian, R. C. Palacharla, V. Benade, N. Muddana, P. Jayarajan, *J. Med. Chem.* **2018**, *61*, 4993.
- [30] S. A. Tabatabai, S. B. Lashkari, M. R. Zarrindast, M. Gholibeikian, A. Shafiee, *Iran. J. Pharm. Res.* **2013**, *12*, 105.
- [31] V. J. Ram, L. Mishra, N. H. Pandey, D. S. Kushwaha, L. A. C. Pieters, A. J. Vlietinck, *J. Heterocycl. Chem.* **1990**, *27*, 351.
- [32] A. Husain, F. J. Ahmad, M. Ajmal, P. Ahuja, *J. Serb. Chem. Soc.* **2008**, *73*, 781.
- [33] A. O. Maslat, M. Abussaud, H. Tashtoush, M. Al-Talib, *Pol. J. Pharmacol.* **2002**, *54*, 55.
- [34] M. Taha, N. H. Ismail, S. Imran, A. Wadood, F. Rahim, S. M. Saad, K. M. Khan, A. Nasir, *Bioorg. Chem.* **2016**, *66*, 117.
- [35] K. Nakagawa, *Biosci. Biotechnol. Biochem.* **2013**, *77*, 900.
- [36] MedChem Designer, Version 3.0, Simulation Plus Inc., California, USA 2014. <http://www.simulations-plus.com>
- [37] P. Zakeri-Milani, H. Tajerzadeh, Z. Islambolchilar, S. Barzegar, H. Valizadeh, *DARU: J. Pharm. Sci.* **2006**, *14*, 164.
- [38] Q. N. Tariq, S. Malik, A. Khan, M. M. Naseer, S. U. Khan, A. Ashraf, M. Ashraf, M. Rafiq, K. Mahmood, M. N. Tahir, Z. Shafiq, *Bioorg. Chem.* **2019**, *84*, 372.
- [39] K. Yamamoto, H. Miyake, M. Kusunoki, S. Osaki, *FEBS J.* **2010**, *277*, 4205.
- [40] Biovia Discovery Studio, Client, V. 16.1.0. 15350, Dassault Systems, San Diego, CA **2017**.
- [41] S. C. Lovell, I. W. Davis, W. B. Arendall III, P. I. W. de Bakker, J. M. Word, M. G. Prisant, J. S. Richardson, D. C. Richardson, *Proteins* **2003**, *50*, 437.
- [42] M. McGann, *J. Comput.-Aided Mol. Des.* **2012**, *26*, 897.
- [43] OEDocking 3.2.0.2, Open Eye Scientific Software, Santa Fe, NM **2017**. <http://www.eyesopen.com>
- [44] P ElmerChem BioDraw Professional (Ver. 15.0.0.106), Cambridge Soft, Waltham, MA **2017**.
- [45] P. C. D. Hawkins, A. G. Skillman, G. L. Warren, B. A. Ellingson, M. T. Stahl, *J. Chem. Inf. Model.* **2010**, *50*, 572.
- [46] OMEGA 2.5.1.4, Open Eye Scientific Software, Santa Fe, NM 1997. <http://www.eyesopen.com>

SUPPORTING INFORMATION

Additional supporting information may be found online in the Supporting Information section.

How to cite this article: Iftikhar M, Shahnawaz, Saleem M, et al. A novel five-step synthetic route to 1,3,4-oxadiazole derivatives with potent α -glucosidase inhibitory potential and their in silico studies. *Arch Pharm Chem Life Sci.* 2019;e1900095. <https://doi.org/10.1002/ardp.201900095>